LONGITUDINAL AND TRANSVERSE COUPLING DYNAMIC PROPERTIES OF A TIMOSHENKO BEAM WITH MASS ECCENTRICITY

Zhiyang Lei, Jinpeng Su and Hongxing Hua

State Key Laboratory of Mechanical System and Vibration, Institute of Vibration Shock & Noise, Shanghai Jiaotong University, Dongchuan Road 800,200240 Shanghai, China
e-mail: leizhiyang@sjtu.edu.cn

Non-uniform mass distribution on the beam section will lead to the coupling between lateral and axial vibration of a beam. Based on Hamilton's principle and spectral element method (SEM), a double-layer Timoshenko beam model is developed to derive the coupled governing equation. The coupling vibration characteristics are investigated. To simulate the mass eccentricity, the densities and thicknesses of the two layers are different. One layer is quite thinner than the other, but its density is larger. So that the influence of stiffness of the thinner layer on the thicker one's is negligible. A corresponding finite element modal is established to verify the SEM model. The mechanism how the coupling is yielded is revealed. The effects of mass non-uniformity on free vibration and forced vibration of the beam with classical and flexible boundary conditions are analyzed. A control method is presented to reduce the vibration subject to longitudinal forces.

1. Introduction

Many researchers concentrate on non-uniform beams with various cross sections, discrete dynamic components and flexible supporting boundary conditions [1-2]. However, very few of them take the mass eccentric into consideration. Yao Xiongliang [3] investigated a method to suppress bending vibration and noise radiation by applying eccentric mass vibration isolation using wave theory. Yang Zhirong [4] studied the longitudinal and transversal nonlinear coupling vibration of ship shafting with axial force on flexible boundary condition.

Laminated composite beams with asymmetrically distributed will lead to the coupling between bending and axial motion [5]. The analysis of laminated beams is based on Symmetry. Thus, the coupling effects are neglected and the transversal motion equations are derived independently [6,7]. Khalili SMR [8] resolved the free vibration of sandwich beams with dynamic stiffness method. Only shear deformation of the core is considered. Lee U [9] and Kerboua M [10] developed a two-layer Euler-Bernoulli beam with a thin layer of piezoelectric materials and smart materials respectively. Coupled equations and active control methods are presented to decrease the transverse response. QH Nguyen [11] and S Lenci [12] build a two-layer beam model considering the interlayer slip. Natural frequencies and mode shapes are computed. The influences of adhesion stiffness on natural frequencies and mode shapes are revealed. High order shear theory is utilized by Y Frostig [13] to examine a two-layer composite beam with partial interaction. The dynamic responses under seismic excitation are presented. Accuracy of results is improved.

This paper focuses on beams with mass eccentric. The coupled equations of motion are yielded based on a two-layer asymmetry Timoshenko beam. Free vibration and forced vibration characteris-

tics are presented using the spectral element method (SEM) [14], which has high frequency accuracy by employing dynamic shape functions. The natural frequencies and mode shapes are computed both in classical and flexible boundary conditions. The influences of mass eccentric distance on coupling properties are investigated. A control method of eccentric loading to reduce the influence of transverse resonance peaks on axial excitation is presented.

2.   Derivation of coupled governing equations

As Fig.1, the total length of the two-layer Timoshenko beam is L. $E_j, \rho_j, h_j, A_j, u_j$ are Yang's modulus, density, height, area and axial displacement of beam j, ($j = 1or2$) respectively. The derivation of the governing equations is based on assumptions as follow:

1，The displacement in the interface is continuous. There is no slip between the two layers.

2，The transverse displacement $v(x,t)$ of both layers is the same and $v(x,t)$ is small enough.

3，The neutral layer of the system remains the same with the neutral layer of beam 1, namely $h_2 << h_1$. The external force is applied on the neutral axis of beam 1.
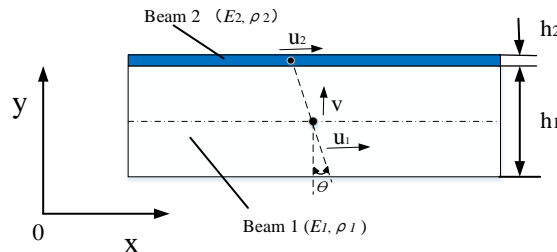

Figure 1. Two-layer Timoshenko beam model.

With the assumptions, the axial displacements of beam 1 and beam 2 subject to:

$$u_2 = u_1 - h\theta / 2 \tag{1}$$

where θ is the rotational displacement, $h = h_1 + h_2$ is the total height of the model.

The axial-transverse coupled dynamic equations of the two-layer beam system are derived with Hamilton's principle. Then, the strain energy of the system can be expressed by

$$V = \frac{1}{2}\int_0^L [E_1A_1u_1'^2 + E_2A_2u_2'^2 + E_1I_1\theta'^2 + E_2I_2\theta'^2 + \kappa G_1A_1(v'-\theta)^2 + \kappa G_2A_2(v'-\theta)^2]dx \tag{2}$$

in which, I_1 and I_2 stand for the area moments of inertia of the beams. κ is the shear factor. G_1 and G_2 denote shear modulus of the beams.

The kinetic energy of the system can be written as follows:

$$T = \frac{1}{2}\int_0^L [\rho_1A_1\dot{u}_1^2 + \rho_2A_2\dot{u}_2^2 + (\rho_1A_1 + \rho_2A_2)\dot{v}^2 + \rho_1I_1\dot{\theta}^2 + \rho_2I_2\dot{\theta}^2]dx \tag{3}$$

The virtual work due to external forces as shown in Fig.2 is given by:

$$\delta W = -N_0(t)\delta u_1(0,t) + N_L(t)\delta u_1(L,t) - M_0(t)\delta\theta(0,t) + M_L(t)\delta\theta(L,t) - Q_0(t)\delta v(0,t) + Q_L(t)\delta v(L,t) \tag{4}$$

where N, M, Q are the axial force, bending moment, and transverse shear force respectively. δu, $\delta\theta$, δv are the virtual displacements separately in axial, rotational and transverse direction.
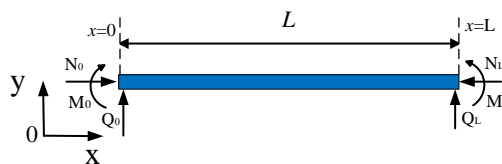

Figure 2. External forces on the ends of the beam.

Based on the Hamilton's principle, the variational equation can be derived as

$$\int_{t1}^{t2} (\delta T - \delta V + \delta W)dt = 0 \tag{5}$$

Then the governing partial equations are established in the following form:

$$EAu_1'' - \rho A\ddot{u}_1 + \alpha\ddot{\theta} - \beta\theta'' = 0$$

$$EI\theta'' - \rho I\ddot{\theta} + \alpha\ddot{u}_1 - \beta u_1'' + \kappa GA(v' - \theta) = 0 \tag{6}$$

$$\kappa GA(v'' - \theta') - \rho A\ddot{v} = 0$$

Meanwhile, the boundary conditions are yielded as:

$$N = EAu_1' - \beta\theta', \quad M = EI\theta' - \beta u_1', \quad Q = \kappa GA(v' - \theta) \tag{7}$$

where the corresponding coefficients can be calculated as:

$$\rho A = \rho_1 A_1 + \rho_2 A_2; \quad \rho I = \rho_1 I_1 + \rho_2 I_2 + \rho_2 A_2 h^2 / 4; \quad EI = E_1 I_1 + E_2 I_2 + E_2 A_2 h^2 / 4;$$

$$EA = E_1 A_1 + E_2 A_2; \quad \kappa GA = \kappa_1 G_1 A_1 + \kappa_2 G_2 A_2; \quad \alpha = \rho_2 A_2 h / 2; \quad \beta = E_2 A_2 h / 2;$$

The governing equations are coupled with coefficients α and β in Eq.(6). α is related to the mass non-uniformity, and β is owed to stiffness non-uniformity.

3. Solution of the coupled equations with spectral element method

The equations can be solved by the method of separation variables. Supposing the harmonic variation for axial, lateral and rotational displacement u_1, v, θ are:

$$u_1 = U(\mathrm{x}, \omega)\mathrm{e}^{i\omega t}, \quad v = V(\mathrm{x}, \omega)\mathrm{e}^{i\omega t}, \quad \theta = \Theta(\mathrm{x}, \omega)\mathrm{e}^{i\omega t} \tag{8}$$

where U, V, Θ are the dynamic shape functions, and ω is the natural frequency of the beam. Substituting Eqs.(8) to Eqs.(6) yields:

$$EAU'' + \rho A\omega^2 U - \alpha\omega^2\Theta - \beta\Theta'' = 0$$

$$EI\Theta'' + \rho I\omega^2\Theta - \alpha\omega^2 U - \beta U'' + \kappa GA(V' - \Theta) = 0 \tag{9}$$

$$\kappa GA(V'' - \Theta') + \rho A\omega^2 V = 0$$

Assume the solutions are in the form of wave number λ:

$$V = Ce^{-i\lambda \mathrm{x}}, U = r_1 Ce^{-i\lambda x}, \Theta = r_2 Ce^{-i\lambda x} \tag{10}$$

By substituting Eqs.(10) to Eqs.(9),the equations become:

$$\begin{bmatrix} 0 & \rho A\omega^2 - \lambda^2 EA & \beta\lambda^2 - \alpha\omega^2 \\ -\eta\lambda i & \beta\lambda^2 - \alpha\omega^2 & \rho I\omega^2 - EI\lambda^2 - \eta \\ \rho A\omega^2 - \eta\lambda^2 & 0 & \eta\lambda i \end{bmatrix} \begin{bmatrix} 1 \\ r_1 \\ r_2 \end{bmatrix} = \begin{bmatrix} 0 \\ 0 \\ 0 \end{bmatrix} \tag{11}$$

where $\eta = \kappa GA$.Since the displacements can't be all zero, the determinant of the coefficient matrix of the homogeneous equation is zero. Then λ can be computed from:

$$\lambda^6 + \alpha_2\lambda^4 + \alpha_3\lambda^2 + \alpha_4 = 0 \tag{12}$$

where

$$\alpha_0 = (\beta^2 - EAEI)\eta; \quad \alpha_2 = \omega^2[EA\rho I\eta - \beta^2\rho A + EI(EA + \eta)\rho A - 2\alpha\beta\eta] / (\alpha_0);$$

$$\alpha_3 = \omega^2[-EI(\rho A\omega)^2 - \rho A(\rho I\omega^2 - \eta)(EA + \eta) + \eta\alpha^2\omega^2 + 2\alpha\beta\rho A\omega^2 - \rho A\eta^2] / (\alpha_0);$$

$$\alpha_4 = \rho A\omega^4[(\rho A\rho I - \alpha^2)\omega^2 - \rho A\eta] / (\alpha_0);$$

Then the corresponding vector $r_1^{(n)}, r_2^{(n)} (n = 1......6)$ can be calculated as:

$$r_2^{(n)} = i\frac{\rho A\omega^2 - \eta\lambda_n^2}{\eta\lambda_n}, r_1^{(n)} = -\frac{\beta\lambda_n^2 - \alpha\omega^2}{\rho A\omega^2 - \lambda_n^2 EA} r_2^{(n)} \tag{13}$$

The dynamic displacement shape functions are composed by coefficient C_n which is related to boundary conditions. The general solutions to Eqs.(10)are given by:

$$U(\mathrm{x}) = \sum_{n=1}^{6} r_1^{(n)} C_n e^{-i\lambda_n x}; V(\mathrm{x}) = \sum_{n=1}^{6} C_n e^{-i\lambda_n x}; \Theta(\mathrm{x}) = \sum_{n=1}^{6} r_2^{(n)} C_n e^{-i\lambda_n x} \tag{14}$$

At the both end of the beam, the displacement can expressed by setting $x = 0$ and $x = L$ in Eqs.(14). The displacements are expressed by:

$$x = 0, U(0) = U_0, V(0) = V_0, \Theta(0) = \Theta_0$$
$$x = L, U(L) = U_L, V(L) = V_L, \Theta(L) = \Theta_L \tag{15}$$

which can be written in matrix form:

$$\begin{bmatrix} U_0 \\ V_0 \\ \Theta_0 \\ U_L \\ V_L \\ \Theta_L \end{bmatrix} = \begin{bmatrix} r_1^{(1)} & r_1^{(2)} & r_1^{(3)} & r_1^{(4)} & r_1^{(5)} & r_1^{(6)} \\ 1 & 1 & 1 & 1 & 1 & 1 \\ r_2^{(1)} & r_2^{(2)} & r_2^{(3)} & r_2^{(4)} & r_2^{(5)} & r_2^{(6)} \\ r_1^{(1)}d_1 & r_1^{(2)}d_2 & r_1^{(3)}d_3 & r_1^{(4)}d_4 & r_1^{(5)}d_5 & r_1^{(6)}d_6 \\ d_1 & d_2 & d_3 & d_4 & d_5 & d_6 \\ r_2^{(1)}d_1 & r_2^{(2)}d_2 & r_2^{(3)}d_3 & r_2^{(4)}d_4 & r_2^{(5)}d_5 & r_2^{(6)}d_6 \end{bmatrix} \begin{bmatrix} C_1 \\ C_2 \\ C_3 \\ C_4 \\ C_5 \\ C_6 \end{bmatrix} = [T_1][C]^T \tag{16}$$

where $d_n = e^{-i\lambda_n L} (n = 1 \ldots \ldots 6)$. At the both ends of the beam, the forces as shown in Fig.2 can be expressed by setting $x = 0$ and $x = L$ in Eqs.(7).

$$x = 0, N(0) = -N_0, Q(0) = -Q_0, M(0) = -M_0$$
$$x = L, N(L) = N_L, Q(L) = Q_L, M(L) = M_L \tag{17}$$

which can be represented in matrix form:

$$[-N_0, -Q_0, -M_0, N_L, Q_L, M_L]^T = [T_2][C_1, C_2, C_3, C_4, C_5, C_6]^T = [T_2][C]^T \tag{18}$$

where the elements of matrix T_2 are as below ($n = 1, 2 \ldots \ldots 6$):

$$T_2(1,n) = [i\lambda_n(EAr_1^{(n)} - \beta r_2^{(n)})]; \quad T_2(2,n) = [\eta(i\lambda_n - r_2^{(n)})]; \quad T_2(3,n) = [i\lambda_n(EIr_2^{(n)} - \beta r_1^{(n)})];$$
$$T_2(4,n) = -[i\lambda_n(EAr_1^{(n)} - \beta r_2^{(n)})]d_n; \quad T_2(5,n) = -[\eta(i\lambda_n - r_2^{(n)})]d_n; \quad T_2(6,n) = -[i\lambda_n(EIr_2^{(n)} - \beta r_1^{(n)})]d_n;$$

Thus, the relation between forces and displacements is derived by eliminating $[C]^T$ from Eqs. (16),(18), which is yielded as:

$$[F] = [ST(\omega)][U] \tag{19}$$

where $[F] = [-N_0, -Q_0, -M_0, N_L, Q_L, M_L]^T$, $[U] = [U_0, V_0, \Theta_0, U_L, V_L, \Theta_L]^T$ and the frequency-dependent spectral element matrix $[ST(\omega)] = [T2][T1]^{-1}$.

On classical boundary conditions, the natural frequencies are determined by

$$\det(ST(\omega_g)) = 0. \tag{20}$$

When ω_g is obtained, the wavenumber λ, coefficient $[C]^T$ and vector $r_1^{(n)}, r_2^{(n)} (n = 1, 2, \ldots, 6)$ are specified and the mode shapes can be obtained from Eqs.(14).

As for flexible boundary conditions, the spectral element matrix is modified as

$ST'(\omega) = ST(\omega) - f_k(\omega)$, where the equivalent boundary forces $f_k = diag\{k_1 U_0, k_3 V_0, k_5 \Theta_0, k_2 U_L, k_4 V_L, k_6 \Theta_L\}$. Now, the natural frequencies and mode shapes can be decided in the same way. The forced responses can be obtained from Eq.(19) when external forces are prescribed.

4. Optimal control method

As Fig.3 shows, the mass center of the system does not coincide with the neutral axis due to geometric asymmetry and ξ is the mass eccentric distance. On this occasion, the loading position is typically coincidental with the geometrical center, which will result in significant coupling responses in both axial and transverse directions based on Eqs.(6). An optimal control method of eccentric loading is raised to decrease the coupled responses under axial excitation. The loading position is adjusted to a certain distance e from stiffness center in height direction. The eccentric distance e is the optimized parameter and the objective function is the displacement response of the beam under
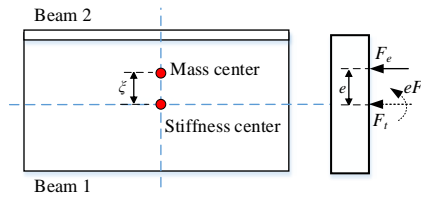
axial eccentric excitations.

Figure 3.Eccentric loading.

When the harmonic excitation force F_e is not located in the stiffness center, it can be equivalent to a harmonic force F_t and harmonic moment eF_t applied to the stiffness center. So the objective function can be written as:

$$[U(x,\omega)] = \min \left\| [ST(\omega)]^{-1} [F] \right\| \tag{21}$$

where $[U]$ is the displacement response vector and $[F] = (F_t, 0, eF_t, 0, 0, 0)^T$ is the eccentric load vector. $[ST(\omega)]^{-1}$ is the inverse matrix of spectral element matrix $ST(\omega)$. This paper is focused on reducing transversal resonance contributions in both axial and transverse responses. Thus, the transverse displacement object function is:

$$V_0(x,\omega) = \min \left| ST^{-1}_{(2,1)} + e \cdot ST^{-1}_{(2,3)} \right| \tag{22}$$

where $ST^{-1}_{(l,j)}$ represents the lth row, the jth column element of the inverse matrix of spectral element matrix. According to Eq.(22), when the minimum displacement occurs, the optimized eccentric distance is:

$$e = -ST^{-1}_{(2,1)} / ST^{-1}_{(2,3)} \tag{23}$$

5. Numerical results and discussion

5.1 Model validation

In order to demonstrate the correctness and accuracy of the analysis method proposed above, a two-layer beam with rectangular cross section is analyzed in different boundary conditions. Meanwhile, a corresponding three dimensional FEM model is established and the characteristics of the system are compared to those of FEM model. The three dimensional model with the same parameters in Table.1 is displayed in Fig.4. The natural frequencies and relative errors in free-free, fix-fix and free-fix boundary conditions are presented in Table.2. Additionally, in Table.2, mode 6th is the 1st axial mode, while others are bending modes. The maximum relative error of natural frequencies is no more than 3% which is acceptable in engineering practice.

Table 1. Calculation parameters of the two-layer beam.

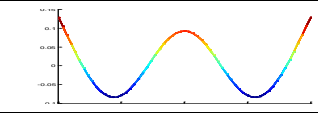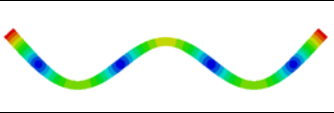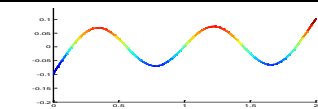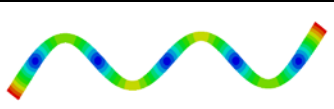| Parameter	$E/(N/m^{-2})$	κ	$h/(m)$	$\rho/(Kg \cdot m^{-3})$	$L/(m)$	$b/(m)$
Beam1	2×10^9	0.849	0.05	2700	2	0.05
Beam2	2×10^9	0.849	0.005	10000	2	0.05
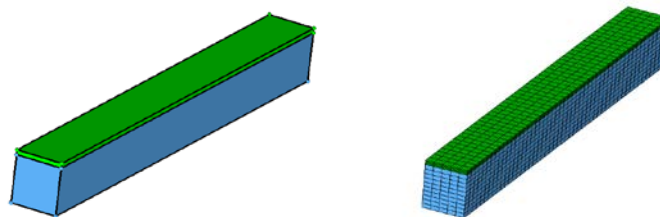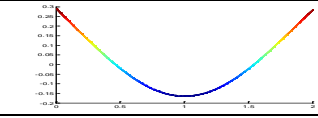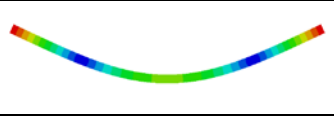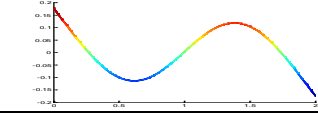
Figure 4.Three dimensional FEM model.

Table 2. Natural frequencies in free-free, fix-fix and free-fix boundary condition.

Modal order	Free-free			Fix-fix			Free-fix		
	Frequency（Hz）		Relative error	Frequency（Hz）		Relative error	Frequency（Hz）		Relative error
	SEM	FEM		SEM	FEM		SEM	FEM	
Mode 1	11.62	11.38	2.1%	11.62	11.36	2.2%	1.75	1.79	2.2%
Mode 2	31.67	31.19	1.5%	31.67	31.11	1.8%	11.46	11.20	2.3%
Mode 3	61.59	60.65	1.5%	61.59	60.40	1.9%	31.67	31.16	1.6%
Mode 4	100.4	99.23	1.2%	100.4	98.69	1.7%	61.43	60.53	1.5%
Mode 5	147.85	146.34	1.1%	147.85	145.40	1.6%	96.44	98.91	-2.5%
Mode 6	193.89	199.57	2.8%	193.89	198.64	2.4%	100.11	101.24	-1.1%
Mode 7	203.08	201.46	0.8%	203.08	199.89	1.5%	147.37	145.88	1.0%
Mode 8	265.47	263.93	0. 8%	265.47	261.53	1.5%	202.30	200.67	0.8%

The first four mode shapes of both the method introduced and FEM model are presented in Table.3.. The results are consistent with the finite element model.

Table 3. Mode shapes in free-free boundary condition.

Modal order	Mode shape	
	SEM	FEM
Mode 1		
Mode 2		
Mode 3		
Mode 4		

Above all, both natural frequencies and mode shapes have a good agreement with FEM models, which illustrates that using our method to evaluate the dynamic properties of the system is reliable and practicable.

5.2 Analysis of coupled dynamic properties

5.2.1 Coupled response

Axial-bending coupled dynamic response is investigated to reveal axial and transverse coupling vibration properties. At the end of the beam, an axial unit harmonic force is applied to excite the beam. The axial response and transverse response of the beam under the excitation are obtained as shown in Fig.5 and Fig.6. Compared to uniform beam, the governing equations shown in Eqs.(6) and boundaries presented in Eqs.(7) are coupled with mass coupling coefficients α and stiffness coupling coefficient β. Thus, longitudinal excitations can stimulate bending modes which lead to the axial displacement responses locally amplification at a certain frequency domain. Longitudinal resonance peaks also can be seen from the lateral response curve.
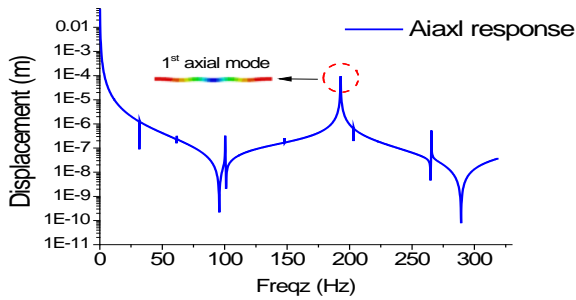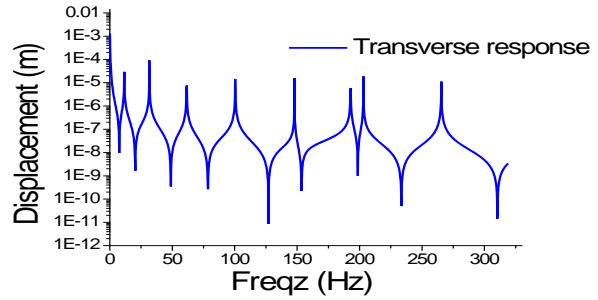
Figure 5. Axial response under axial excitation.　　**Figure 6.** Lateral response under axial excitation.

5.2.2 The influence of the mass eccentric distance

Figure.7 shows the natural frequencies stay almost the same with the increasing mass eccentric distance ξ which is related to the density of the beams. The variation of mass eccentric distance follows the principle that the total mass of the system stays the same. However, the dynamic responses change a lot with different eccentric distance. In the system, beam 1 plays a major role in natural frequency property that is in accord with assumptions while beam 2 plays a role of transferring energy which leads to the coupling between axial vibrations and bending vibration. When ξ rises, the frequencies which are mainly determined by beam 1 remains the same. Meanwhile the mass coupling coefficient α increases and that strengthens the coupling between axial and transverse vibration.
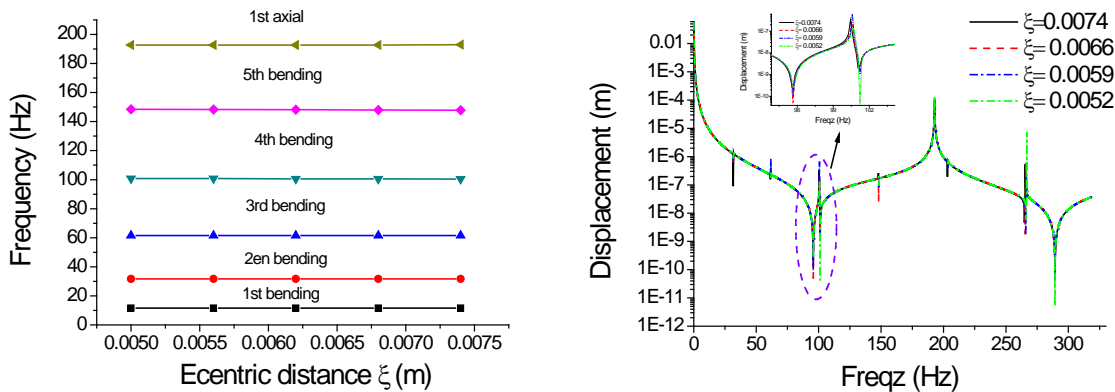

Figure 7. Influence of mass eccentric distance.

5.3 Investigation on optimization

Based on Eq.(23)The eccentric distance e is concerned with frequency. Fig.9 shows the optimized eccentric loading distance varies with frequency. The optimization responses can be obtained in a certain frequency range. For example, to minimize the transverse response between frequency 75Hz and 125Hz, the optimized eccentric distance is determined by Eq.(23) and showed in Fig.9 which is $e = 0.003$. The optimized responses are presented in Fig.10. After optimization, the contribution of bending modes in lateral response and axial response curves are supressed in the certain frequency range. The optimized method is effective and useful.
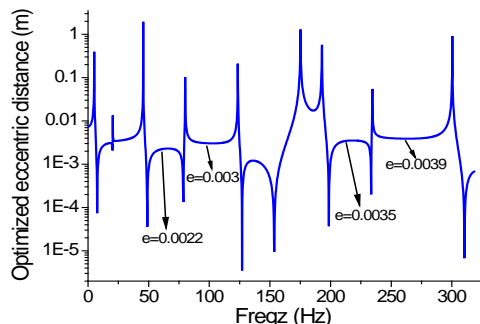

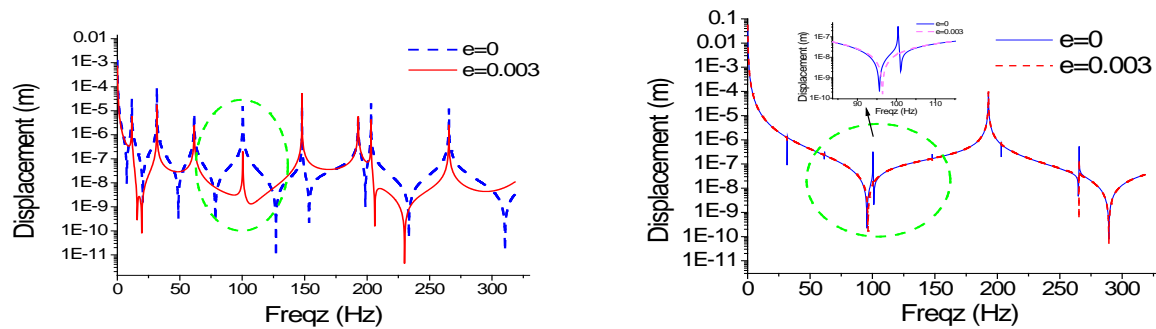**Figure 8.** Optimized eccentric loading distance.

Figure 9. Transverse and axial response optimized at 75Hz-125Hz, $e = 0.003$.

6. Conclusion

In this paper, a two-layer asymmetry Timoshenko beam model is established to simulate a beam with mass eccentric. The axial and bending coupled vibration governing equations and boundary conditions are yielded using Hamilton's principle. Spectral element method is applied to solve the equations in different boundary conditions. Natural frequencies, mode shapes and coupled responses are computed from the equations. The results are consistent with the corresponding three dimensional finite element models'. The coupled controlling equations reveal that axial excitation can stimulate bending modes, which will lead to the axial and transverse response locally amplification. Different mass eccentric models show no significant changes on natural frequencies which indicates beam 1 plays major role in natural frequencies, while beam 2 contributes to energy transferring leading to the coupling vibration. To minimize coupled transverse response, an optimal control method of eccentric loading is raised to decrease the response under axial excitation. The optimal eccentric loading distance is presented and the optimized responses are obviously reduced in a certain frequency range.

REFERENCES

1   Li W L. Free vibrations of beams with general boundary conditions [J]. Journal of Sound and Vibration, 2000, 237(4): 709-725.
2   Wu J J, Whittaker A R. The natural frequencies and mode shapes of a uniform cantilever beam with multiple two-dof spring–mass systems [J]. Journal of Sound and Vibration, 1999, 227(2): 361-381.
3   Yao X L, Ji F, Qian D J. Characteristics of eccentric blocking masses attenuating vibration wave propagation [J]. Journal of Vibration and Shock, 2010, 29(1): 48-52.
4   Yang Z R , Zou D, Rao Z S et al. Responses of Longitudinal and Transversal Nonlinear Coupling Vibration of Ship Shafting[J]. Journal of Ship Mechanics, 2014 (12).
5   Della C N, Shu D. Vibration of delaminated composite laminates: A review [J]. Applied Mechanics Reviews, 2007,60(1): 1-20.
6   Lee J. Free vibration analysis of delaminated composite beams [J]. Computers & Structures, 2000, 74(2): 121-129.
7   Hajianmaleki M, Qatu M S. Vibrations of straight and curved composite beams: a review [J]. Composite Structures, 2013, 100: 218-232.
8   Khalili S M R, Nemati N, Malekzadeh K, et al. Free vibration analysis of sandwich beams using improved dynamic stiffness method[J]. Composite Structures, 2010, 92(2): 387-394.
9   Lee U, Kim J. Dynamics of elastic-piezoelectric two-layer beams using spectral element method [J]. International Journal of Solids and Structures, 2000, 37(32): 4403-4417.
10 Kerboua M, Megnounif A, Benguediab M, et al. Vibration control beam using piezoelectric-based smart materials[J]. Composite Structures, 2015, 123: 430-442.
11 Nguyen Q H, Hjiaj M, Le Grognec P. Analytical approach for free vibration analysis of two-layer Timoshenko beams with interlayer slip[J]. Journal of Sound and Vibration, 2012, 331(12): 2949-2961.
12 Lenci S, Clementi F. Effects of shear stiffness, rotatory and axial inertia, and interface stiffness on free vibrations of a two-layer beam[J]. Journal of Sound and Vibration, 2012, 331(24): 5247-5267.
13 Frostig Y, Baruch M, Vilnay O, et al. High-order theory for sandwich-beam behavior with transversely flexible core[J]. Journal of Engineering Mechanics, 1992, 118(5): 1026-1043.
14 Lee U. *Spectral element method in structural dynamics* [M]. John Wiley & Sons, 2009.